7-10-2018

HST Follow-up Observations of Two Bright z ∼ 8 Candidate Galaxies from the BoRG Pure-parallel Survey

R. C. Livermore
University of Melbourne

M. Trenti
University of Melbourne

L. D. Bradley
STScI

S. R. Bernard
University of Melbourne

Benne W. Holwerda
University of Louisville, benne.holwerda@louisville.edu

See next page for additional authors

Draft version July 5, 2018
Typeset using LaTeX **twocolumn** style in AASTeX61

HST FOLLOWUP OBSERVATIONS OF TWO BRIGHT $z \sim 8$ CANDIDATE GALAXIES FROM THE BoRG PURE-PARALLEL SURVEY

R. C. Livermore,[1,2] M. Trenti,[1,2] L. D. Bradley,[3] S. R. Bernard,[1] B. W. Holwerda,[4] C. A. Mason,[5] and T. Treu[5]

[1] *School of Physics, The University of Melbourne, VIC 3010, Australia*
[2] *ARC Centre of Excellence for All Sky Astrophysics in 3 Dimensions (ASTRO 3D)*
[3] *Space Telescope Science Institute, 3700 San Martin Drive, Baltimore, MD 21218, USA*
[4] *Department of Physics and Astronomy, University of Louisville, Louisville, KY 40292, USA*
[5] *Department of Physics and Astronomy, University of California, Los Angeles, CA 90095, USA*

ABSTRACT

We present follow-up imaging of two bright ($L > L^*$) galaxy candidates at $z \gtrsim 8$ from the Brightest of Reionizing Galaxies (BoRG) survey with the F098M filter on the *Hubble Space Telescope*/Wide Field Camera 3 (*HST*/WFC3). The F098M filter provides an additional constraint on the flux blueward of the spectral break, and the observations are designed to discriminate between low- and high-z photometric redshift solutions for these galaxies. Our results confirm one galaxy, BoRG_0116+1425_747, as a highly probable $z \sim 8$ source, but reveal that BoRG_0116+1425_630 - previously the brightest known $z > 8$ candidate ($m_{\rm AB} = 24.5$) - is likely to be a $z \sim 2$ interloper. As this source was substantially brighter than any other $z > 8$ candidate, removing it from the sample has a significant impact on the derived UV luminosity function in this epoch. We show that while previous BoRG results favored a shallow power-law decline in the bright end of the luminosity function prior to reionization, there is now no evidence for departure from a Schechter function form and therefore no evidence for a difference in galaxy formation processes before and after reionization.

Keywords: galaxies: high-redshift — galaxies: luminosity function, mass function — dark ages, reionization, first stars

Corresponding author: R. C. Livermore
rlivermore@unimelb.edu.au

1. INTRODUCTION

The unprecedented sensitivity of the Wide Field Camera 3 (WFC3) on the *Hubble Space Telescope* (*HST*) has provided new insight into the build-up of galaxies during the epoch of reionization ($z \gtrsim 7$; Bouwens et al. 2011, 2015; McLure et al. 2013; Atek et al. 2015; Finkelstein et al. 2015; Ishigaki et al. 2015; Livermore et al. 2017). The picture that has emerged from these observations is that the UV luminosity function is well described by a Schechter function at least out to $z \sim 7$ with the characteristic luminosity and normalization decreasing and the faint-end slope becoming steeper with increasing redshift (e.g. Finkelstein 2016).

Before the completion of reionization, though, the limited sample sizes mean that the picture is less clear. A key remaining question is whether the UV luminosity function continues to show an exponential cut-off at the bright end (e.g. Bradley et al. 2012; Schmidt et al. 2014; Bouwens et al. 2015) or whether it can be described by a power law (e.g. Bowler et al. 2014, 2015, 2017; Finkelstein et al. 2015; Calvi et al. 2016).

Results from semi-analytic models and observations have shown that the break at the bright end of the luminosity function can be interpreted as evidence for quenching due to feedback from active galactic nuclei (AGNs; Bower et al. 2006; Croton et al. 2006) or some other mass-quenching law (Peng et al. 2010), or the build-up of dust in the brightest galaxies (Rogers et al. 2014). Studies have shown that the impact of magnification bias, which might conceal an exponential break, is negligible for current surveys (Barone-Nugent et al. 2015; Mason et al. 2015b). Therefore, if the exponential break is not seen at higher redshifts, this might indicate that the feedback processes are less efficient prior to the completion of reionization, or that brighter galaxies have not yet built up the requisite dust content (e.g. Driver et al. 2017).

In addition to providing insight into the feedback processes affecting galaxy evolution, the UV luminosity function can also provide a view of the overall evolution of star formation in the universe. The integral of the UV luminosity function is related to the cosmic star formation rate density, which is known to increase with redshift up to around $z \sim 2$ and then decline (e.g. Madau et al. 1996; Madau & Dickinson 2014). Studies of the decline beyond $z \sim 8$ have had conflicting results, with some recent work suggesting a smooth decline at $z > 8$ (Ellis et al. 2013; McLeod et al. 2016), while others favor a transition to a much steeper decline (Oesch et al. 2014, 2015). Resolving this tension is vital both for constraining models of galaxy evolution and for accurately predicting expected detections of high-redshift galaxies with the *James Webb Space Telescope* (*JWST*).

The Brightest of Reionizing Galaxies (BoRG) survey (PI: M. Trenti; Trenti et al. 2011) uses pure-parallel observations with *HST*/WFC3 to obtain random pointings across the sky, resulting in coverage over a wide area that is designed to search for rare, bright objects at high redshift. The first results of the BoRG[z9-10] survey revealed five candidate galaxies at $8.3 < z < 10$, including the brightest known candidate at $z > 8$ (Calvi et al. 2016, hereafter C16). This galaxy exhibits a strong spectral break in the F105W filter, suggesting a redshift of $z > 8$. However, C16 find a $\sim 10\%$ probability that this is instead a 4000 Å break at $z \sim 1.8$. If confirmed to be at $z > 8$, this brightest candidate with $M_{\rm UV} = -22.8$ (apparent H-band magnitude $m_{H160} = 24.5$) would provide strong evidence in favor of an excess of galaxies at the bright end of the UV luminosity function, lending support to a power-law decline as opposed to the exponential cut-off.

In this Letter, we present follow-up observations with *HST* to confirm the high-redshift nature of this brightest candidate, which also cover a second source in the same field discovered by C16. We describe the observations and data reduction in Section 2, and re-derive the photometric redshift of the two high-z candidates in Section 3. In Section 4 we present the revised UV luminosity function at $z \sim 9$, and we summarize our conclusions in Section 5. Throughout, magnitudes are given according to the AB system (Oke & Gunn 1983) and we adopt a Planck Collaboration et al. (2016) ΛCDM cosmology.

2. OBSERVATIONS AND DATA REDUCTION

The design of the BoRG[$z9-10$] survey (Program ID: 13767; PI: M. Trenti) is described in C16. Briefly, it comprises 480 orbits of pure-parallel imaging of independent lines of sight with the near-IR WFC3 filters F105W, F125W, F140W, and F160W, as well as the long-pass optical filter F350LP. The large area and medium depth (5σ point-source sensitivity of $m_{\rm AB} \sim 26.5-27.5$) is designed to constrain the bright end of the UV luminosity function at $z > 8$ by identifying bright galaxy candidates through broadband photometry.

In order to follow-up the bright $z > 8$ candidate BoRG_0116+1425_630 discovered by C16, an additional orbit was acquired in Cycle 24 (Program ID: 14701; PI: M. Trenti) with the F098M filter.

In the same field as BoRG_0116+1425_630 is another $z > 8$ candidate, BoRG_0116+1425_747, which has additional archival *HST*/Advanced Camera for Surveys

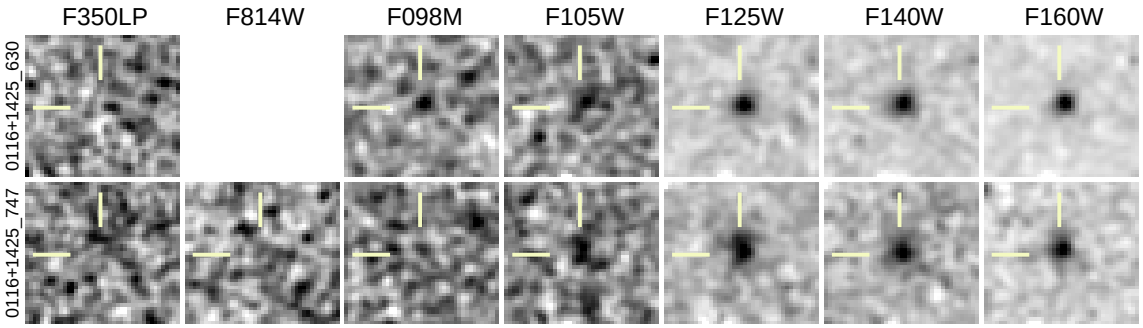

Figure 1. Postage stamp images of the two high-z candidates, BoRG_0116+1425_630 (upper) and BoRG_0116+1425_747 (lower) in each filter. Each image is centered on the source and measures $3\farcs2 \times 3\farcs2$. Note that there is no F814W coverage of BoRG_0116+1425_630.

Table 1. High-z candidates in the BoRG_0116+1425 field

ID	α(J2000)	δ(J2000)	AB Magnitude[a]							z
	(degree)	(degree)	F350LP	F814W	F098M	F105W	F125W	F140W	F160W	
BoRG_0116+1425_630	19.0347	14.4026	> 28.58[b]	···	26.79 ± 0.33	26.88 ± 0.34	25.38 ± 0.08	25.08 ± 0.07	24.81 ± 0.06	1.8
BoRG_0116+1425_747	19.0372	14.4068	> 28.78[c]	> 28.46[d]	> 28.21[e]	27.00 ± 0.32	25.97 ± 0.11	25.98 ± 0.13	25.70 ± 0.10	7.9

[a] Magnitudes are isophotal fluxes from SExtractor FLUX_ISO. For reference, the total magnitudes in F160W for the two sources (from MAG_AUTO) are 24.48 ± 0.06 and 25.04 ± 0.10 for 0116+1425_630 and 0116+1425_747 respectively. Measured fluxes for values given as upper limits are: [b] 4 ± 13 nJy; [c] 10 ± 11 nJy; [d] 10 ± 15 nJy; [e] 18 ± 19 nJy.

Note—Coordinates and magnitudes of the two high-z candidates discovered by C16 in the BoRG_0116+1425 field. Columns 2-3 give the α and δ coordinates in degrees. Columns 4-10 give the magnitude (from SExtractor FLUX_ISO) in each band (note there is no F814W coverage of BoRG_0116+1425_630). For non-detections, we quote the 1σ uncertainty as an upper limit. The redshift z in column 11 is the photometric redshift obtained from BPZ as described in the text.

(ACS) coverage in the F814W filter (Program ID: 14652; PI: B. W. Holwerda).

The calibrated data were downloaded from the Mikulski Archive for Space Telescopes (MAST), where individual exposures had been processed through the standard calibration software to apply bias correction (ACS and WFC3/UVIS), dark subtraction, flat-fielding, and charge-transfer efficiency (CTE) correction (ACS and WFC3/UVIS). As with previous BoRG analyses (Bradley et al. 2012; Schmidt et al. 2014; Bernard et al. 2016; C16), we applied Laplacian edge filtering (van Dokkum 2001) to the WFC3 data to remove residual cosmic rays and detector artifacts such as unflagged hot pixels. Additionally, we corrected the WFC3/UVIS F350LP data for electronic crosstalk (Suchkov & Baggett 2012). The individual exposures in each filter were combined using AstroDrizzle to produce the final science images and their associated inverse-variance weight maps. Like previous BoRG analyses (e.g. Trenti et al. 2011; Bradley et al. 2012; Schmidt et al. 2014; Bernard et al. 2016; Calvi et al. 2016), the images were drizzled to a final pixel scale of $0\farcs08$/pixel. The total exposures times of the combined images were 2095 s, 5207 s, 2612 s, 2209 s, 2059 s, 1759 s, 2409 s in the F350LP, F814W, F098M, F105W, F125W, F140W, and F160W filters, respectively.

One limitation of pure-parallel observations is that they are not dithered, in order to avoid conflict with the primary observation. Accordingly, the design of the BoRG[$z9-10$] survey is optimized to mitigate the impact of the lack of dithering as far as possible. C16 give a full list of the steps taken (their Section 2) and a comparison between undithered pure-parallel data and overlapping dithered data showing that the impact on photometry is negligible (their §3.1). We also note that star/galaxy separation is reliable down to approximately a magnitude above the photometric limit (Holwerda et al. 2014).

For the new data (F814W and F098M), we derived variance maps (rms) from the inverse-variance weight maps (wht) as rms $= 1/\sqrt{\text{wht}}$. Slight correlation between pixels results in the weight maps underestimating the rms, so we rescale them by measuring photometry in empty apertures and normalizing the entire image by a

constant factor such that the median error on the fluxes of empty apertures matches the variance of the sky flux measurements (see Trenti et al. 2011). The normalization factors were 1.24 in F814W and 1.10 in F098M; for the pre-existing images analyzed by C16 they range from 1.06 in F160W to 1.33 in F350LP. These noise measurements also allow us to derive 5σ limiting magnitudes in these two filters of $m_{\rm AB} = 26.60$ and 26.37, respectively (for limiting magnitudes in the other filters, see C16, Table 1).

3. HIGH-z CANDIDATES

We constructed source catalogs using SOURCE EXTRACTOR (SExtractor; Bertin & Arnouts 1996) in dual image mode, using a combined F140W and F160W image and corresponding combined weight map as the detection image. The SExtractor parameters were chosen to match those of C16, so we require nine contiguous pixels with signal-to-noise ratio (S/N)$>$ 0.7. We corrected the fluxes for foreground Galactic extinction $E(B-V) = 0.0349$ (Schlafly & Finkbeiner 2011), and following previous BoRG work (see Trenti et al. 2012) we adopt the isophotal flux (FLUX_ISO) for measuring colors, and define the signal-to-noise as S/N = FLUX_ISO/FLUXERR_ISO. From this final catalog, we select the two high-z candidates from C16 and confirm that the same magnitudes are derived in all of the pre-existing filters. Postage stamp images of the two sources, BoRG_0116+1425_630 and BoRG_0116+1425_747 are shown in Figure 1, and the positions and magnitudes are given in Table 1.

C16 rely on a Lyman-break selection to identify high-z candidate galaxies, but it is nonetheless instructive to use photometric redshift codes to visualize the probability distribution of the redshift of the sources. We use the BPZ code (Benítez 2000; Coe et al. 2006) both with and without the new F098M (and, for BoRG_0116+1425_747, F814W) data, and the results are shown in Figure 2. Both candidates show a break in the F105W filter, which, if interpreted as the Lyman break, places them at redshift $z \gtrsim 8$. In both cases, a secondary solution exists at $z < 2$, in the case where the break is instead the 4000 Å break. As shown in Figures 2 and 3, the addition of the F098M filter helps to distinguish between these two solutions as flux can be measured blueward of the shallower 4000 Å break, but not the steeper Lyman break.

Figures 2 and 3 suggest that BoRG_0116+1425_630 is more likely to be a $z < 2$ contaminant, due to a $3\,\sigma$ detection in the F098M filter; the integral of the $P(z)$ contained in the low-z solution has increased from 31% prior to the addition of F098M, to 96% afterwards. Meanwhile, BoRG_0116+1425_747, with signal-to-noise S/N$<$ 1 in F098M, now has a stronger probability (99%, compared to 64% previously) of being a $z \sim 8$ galaxy (an independent analysis with another photometric redshift code confirms the $z \sim 8$ solution in the latter case; Bridge et al. 2018, in preparation). With the addition of the new data, the secondary solutions encompass a negligible fraction of the probability distribution: 4% for BoRG_0116+1425_630 and 1% for BoRG_0116+1425_747. The best-fitting photometric redshifts are now $1.80^{+0.15}_{-0.10}$ and $7.87^{+0.29}_{-0.23}$ for BoRG_0116+1425_630 and BoRG_0116+1425_747 respectively, where the uncertainties include the central 68% of the probability distribution. We note that adding the new data does not change the redshift of the high-z peak of the redshift probability distribution in either case (to within the $\Delta z = 0.1$ resolution used in the fit). The low-z peak for BoRG_0116+1425_630 is also unchanged, but the secondary solution for BoRG_0116+1425_747 has increased from $z = 1.45$ to $z = 1.73$.

We can also modify the Lyman-break selection method used by C16 to incorporate the new data. These criteria require strong (S/N$>$ 4) detections in each filter redward of the Lyman break, with a relatively flat spectrum in this region ($JH_{140} - H_{160} < 0.3$), and a clear break in a pair of adjacent filters ($Y_{105} - JH_{140} > 1.5$ and $Y_{105} - JH_{140} > 5.33 \cdot (JH_{140} - H_{160}) + 0.7$), with a non-detection (S/N$<$ 1.5) blueward of the break. A cut of S/N$\geq$ 8 is also required in the detection image. Both of the candidates were previously selected to meet these criteria (see C16 for full details). To this, we can add a requirement for S/N$<$ 1.5 in the F098M filter, as well as F814W for BoRG_0116+1425_747. With S/N$\sim$ 3 in F098M, BoRG_0116+1425_630 does not meet the new criteria and is therefore removed from the $z \sim 9$ sample. However, BoRG_0116+1425_747 has S/N$<$ 1 in both F814W and F098M, and so would still be selected in the $z \sim 8$ sample.

Using the available photometry, we can derive some physical characteristics of the two galaxies. We use the Fitting and Assessment of Synthetic Templates (FAST) code (Kriek et al. 2009) with Bruzual & Charlot (2003) stellar population synthesis models, a Chabrier (2003) initial mass function, a Calzetti et al. (2000) dust attenuation law and a delayed exponential star formation history. Assuming that BoRG_0116+1425_630 has the best-fitting redshift of $z \sim 1.8$, it is undetected in the rest-frame ultraviolet, giving an upper limit on the star formation rate of $\log(\mathrm{SFR}/\mathrm{M}_\odot\,\mathrm{yr}^{-1}) < 0.47$, and we find a stellar mass $\log(M_*/M_\odot) = 9.93^{+0.28}_{-0.25}$. For BoRG_0116+1425_747, assuming $z \sim 7.9$,

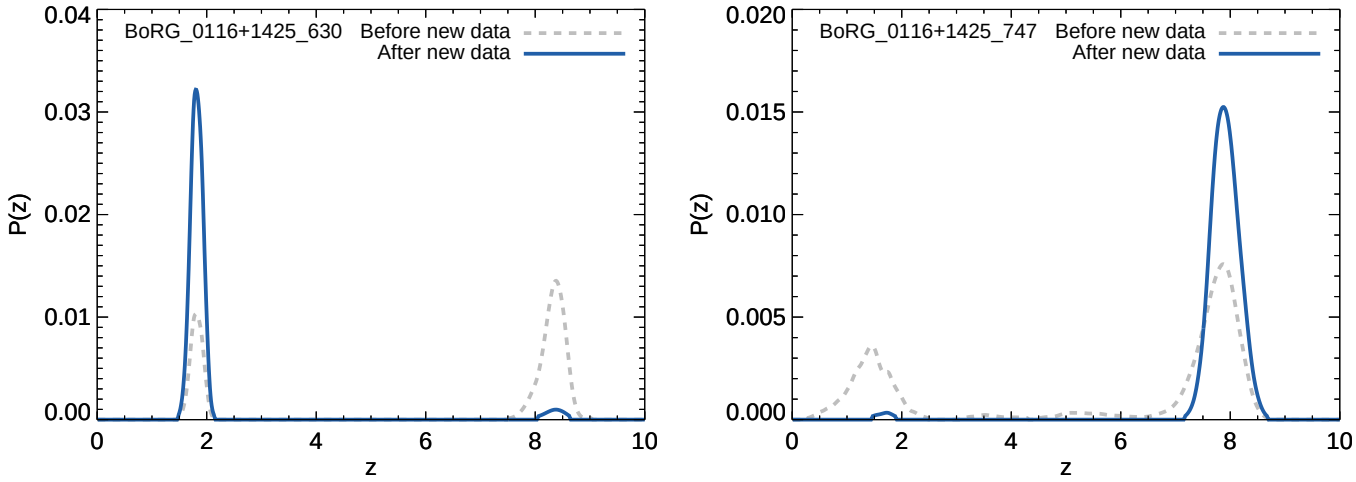

Figure 2. Photometric redshift probability distribution ($P(z)$) obtained from BPZ with a flat prior. The gray dashed line indicates the $P(z)$ obtained before adding the new data, indicating the degeneracy of the $z \gtrsim 8$ and $z < 2$ solutions. The solid blue line shows the result after adding the F098M (and, for BoRG_0116+1425_747, F814W) imaging. The new addition of the new data causes the $P(z)$ to converge on one solution; a lower redshift $z \sim 1.8$ is now preferred for BoRG_0116+1425_630, whereas BoRG_0116+1425_747 remains likely to be at $z \sim 8$ with a higher probability.

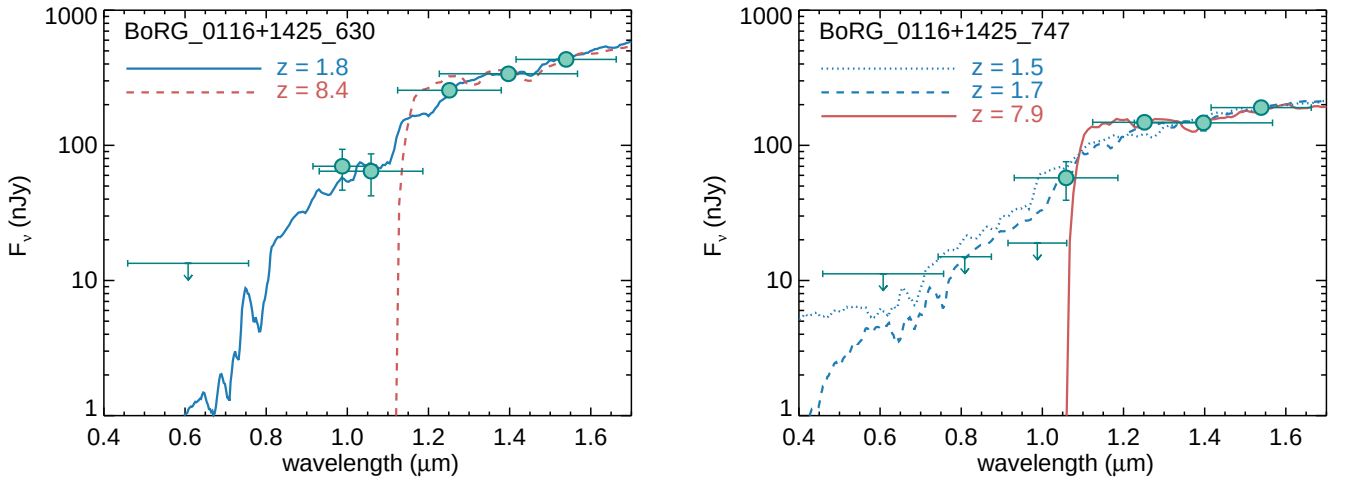

Figure 3. Best-fit spectral energy distributions (SEDs) for the two sources at each of the peaks in the photometric redshift probability distribution. For BoRG_0116+1425_747 we show both the low-z solution before adding the new data ($z \sim 1.5$) and that from after adding the new data ($z \sim 1.7$). In all other cases, the SED fits are identical before and after adding the new data. The F098M filter acts as a key differentiator between the low- (blue) and high- (red) redshift solutions. The SED preferred after adding the new data is indicated by a solid line.

we find $M_{\rm UV} = -22.0$ and a star formation rate $\log(\mathrm{SFR}/\mathrm{M}_\odot\,\mathrm{yr}^{-1}) = 1.13^{+1.28}_{-0.52}$.

4. THE UV LUMINOSITY FUNCTION AT $z \sim 9$

The new data presented in this Letter indicate that the $z \sim 9$ candidate BoRG_0116+1425_630 is a low-z interloper. Due to its bright nature, the removal of this single source from the $z \sim 9$ BoRG sample has a significant effect on the derived luminosity function. With a derived absolute magnitude at $z \sim 9$ of $M_{\rm AB} = -22.8$, it would be extremely rare if the UV luminosity function were to remain Schechter-like in this epoch with an exponential cut-off at the bright end. Based on the theoretical prediction of the evolution of the UV luminosity function of Mason et al. (2015a), the probability of finding a galaxy at this magnitude in the BoRG data would be $p = 2.8 \times 10^{-3}$. According to the empirically derived luminosity function of Finkelstein (2016), it would be even rarer, with a probability of $p = 5.4 \times 10^{-5}$. Therefore, had this candidate been confirmed, it would therefore have been strong evidence in favor of a departure from a Schechter function in this epoch.

As we have shown that this galaxy is likely to be a $z \sim 2$ interloper, we revise the luminosity function

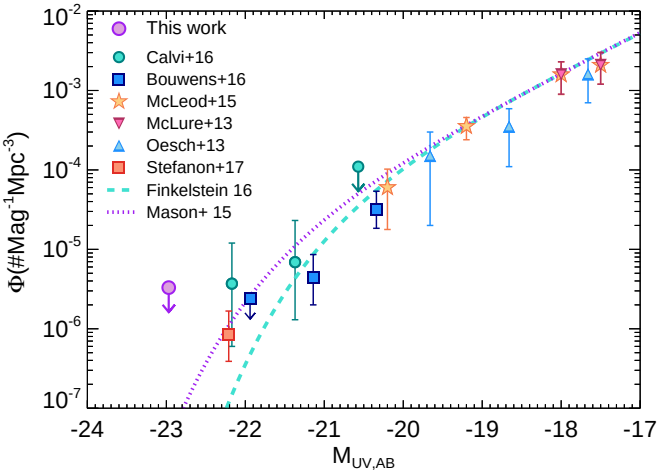

Figure 4. The $z \sim 9$ luminosity function after the low-z contaminant BoRG_0116+1425_630 is removed. Removing this bright source means that the excess at the bright end presented by C16 becomes an upper limit, which is now consistent with the theoretical prediction of Mason et al. (2015a). Additional observational data are shown from McLure et al. (2013), Oesch et al. (2013), Bouwens et al. (2016), McLeod et al. (2016), and Stefanon et al. (2017).

to exclude this candidate. Full details of the computation of the luminosity function are provided in C16; in Figure 4 we show the result of removing this single source. There are now no known sources at $z > 8$ with $M_{\rm AB} < -22.5$, and the observations are now consistent with the predicted Schechter function of Mason et al. (2015a). This means that there is no evidence that the process of galaxy evolution differs before and after reionization. However, we note that while the BoRG data now do not favor a power-law form to the bright end of the luminosity function, nor do they rule it out. There remains tentative evidence that a power law is preferred at $z \sim 7$ (Bowler et al. 2017), and at $z \sim 8$ it has been shown to fit equally as well as a Schechter function (Finkelstein et al. 2015). Further data over a wider area, such as the forthcoming BoRG[4JWST] survey, will be required to constrain the number density of the brightest galaxies in this epoch.

5. CONCLUSIONS

We have presented follow-up imaging of two bright high-z galaxy candidates with the F098M filter on *HST*/WFC3. Both galaxies were selected as $z \gtrsim 8$ candidates in the BoRG survey based on strong detections in the near-infrared and non-detections in the optical F350LP filter. The addition of another filter blueward of the break confirms BoRG_0116+1425_747 as a probable $z \sim 8$ source, but reveals that BoRG_0116+1425_630 - previously the brightest known $z > 8$ candidate - is likely to be a $z \sim 2$ interloper.

The removal of BoRG_0116+1425_630 from the $z > 8$ sample strongly affects the conclusions about the UV luminosity function in this epoch. Previously, the BoRG results of C16 supported a transition from an exponential decline at the bright end after reionization to a shallower power-law decline beforehand. Removing this bright source from the sample means that there is now no evidence for a departure from the Schechter function, and therefore no evidence for difference in the galaxy formation process before and after reionization.

These results highlight the usefulness of the F098M filter for identifying $z < 2$ interlopers in Lyman Break-selected samples, and further demonstrates the need for large high-z surveys to constrain the bright end of the luminosity function prior to the launch of *JWST*.

The authors would like to thank the anonymous referee for helpful comments that clarified the text of this Letter. This work is based on observations made with the NASA/ESA Hubble Space Telescope, which is operated by the Association of Universities for Research in Astronomy, Inc., under NASA contract NAS 5-26555. We acknowledge support by NASA through grant HST-GO-14701. Parts of this research were supported by the Australian Research Council Centre of Excellence for All Sky Astrophysics in 3 Dimensions (ASTRO 3D), through project number CE170100013. R.C.L. acknowledges support from an Australian Research Council Discovery Early Career Researcher Award (DE180101240).

REFERENCES

Atek, H., Richard, J., Jauzac, M., et al. 2015, The Astrophysical Journal, 814, 69

Barone-Nugent, R. L., Wyithe, J. S. B., Trenti, M., et al. 2015, MNRAS, 450, 1224

Benítez, N. 2000, The Astrophysical Journal, 536, 571

Bernard, S. R., Carrasco, D., Trenti, M., et al. 2016, The Astrophysical Journal, 827, 76

Bertin, E., & Arnouts, S. 1996, Astronomy and Astrophysics Supplement, 117, 393

Bouwens, R. J., Illingworth, G. D., Oesch, P. A., et al. 2011, The Astrophysical Journal, 737, 90

—. 2015, The Astrophysical Journal, 803, 34

Bouwens, R. J., Oesch, P. A., Labbe, I., et al. 2016, The Astrophysical Journal, 830, 67

Bower, R. G., Benson, A. J., Malbon, R., et al. 2006, MNRAS, 370, 645
Bowler, R. A. A., Dunlop, J. S., McLure, R. J., & McLeod, D. J. 2017, MNRAS, 466, 3612
Bowler, R. A. A., Dunlop, J. S., McLure, R. J., et al. 2014, MNRAS, 440, 2810
—. 2015, MNRAS, 452, 1817
Bradley, L. D., Trenti, M., Oesch, P. A., et al. 2012, The Astrophysical Journal, 760, 108
Bruzual, G., & Charlot, S. 2003, MNRAS, 344, 1000
Calvi, V., Trenti, M., Stiavelli, M., et al. 2016, The Astrophysical Journal, 817, 120
Calzetti, D., Armus, L., Bohlin, R. C., et al. 2000, The Astrophysical Journal, 533, 682
Chabrier, G. 2003, The Publications of the Astronomical Society of the Pacific, 115, 763
Coe, D., Benítez, N., Sánchez, S. F., et al. 2006, The Astronomical Journal, 132, 926
Croton, D. J., Springel, V., White, S. D. M., et al. 2006, MNRAS, 365, 11
Driver, S. P., Andrews, S. K., da Cunha, E., et al. 2017, arXiv, arXiv:1710.06628
Ellis, R. S., McLure, R. J., Dunlop, J. S., et al. 2013, The Astrophysical Journal Letters, 763, L7
Finkelstein, S. L. 2016, Publications of the Astronomical Society of Australia, 33, 37
Finkelstein, S. L., Ryan, R. E. J., Papovich, C., et al. 2015, The Astrophysical Journal, 810, 71
Holwerda, B. W., Trenti, M., Clarkson, W., et al. 2014, The Astrophysical Journal, 788, 77
Ishigaki, M., Kawamata, R., Ouchi, M., et al. 2015, The Astrophysical Journal, 799, 12
Kriek, M., van Dokkum, P. G., Labbé, I., et al. 2009, The Astrophysical Journal, 700, 221
Livermore, R. C., Finkelstein, S. L., & Lotz, J. M. 2017, The Astrophysical Journal, 835, 113
Madau, P., & Dickinson, M. 2014, Annual Review of Astronomy and Astrophysics, 52, 415
Madau, P., Ferguson, H. C., Dickinson, M. E., et al. 1996, MNRAS, 283, 1388
Mason, C. A., Trenti, M., & Treu, T. 2015a, The Astrophysical Journal, 813, 21
Mason, C. A., Treu, T., Schmidt, K. B., et al. 2015b, The Astrophysical Journal, 805, 79
McLeod, D. J., McLure, R. J., & Dunlop, J. S. 2016, MNRAS, 459, 3812
McLure, R. J., Dunlop, J. S., Bowler, R. A. A., et al. 2013, MNRAS, 432, 2696
Oesch, P. A., Bouwens, R. J., Illingworth, G. D., et al. 2015, The Astrophysical Journal, 808, 104
—. 2013, The Astrophysical Journal, 773, 75
—. 2014, The Astrophysical Journal, 786, 108
Oke, J. B., & Gunn, J. E. 1983, Astrophysical Journal, 266, 713
Peng, Y.-j., Lilly, S. J., Kovač, K., et al. 2010, The Astrophysical Journal, 721, 193
Planck Collaboration, Ade, P. A. R., Aghanim, N., et al. 2016, Astronomy & Astrophysics, 594, A13
Rogers, A. B., McLure, R. J., Dunlop, J. S., et al. 2014, MNRAS, 440, 3714
Schlafly, E. F., & Finkbeiner, D. P. 2011, The Astrophysical Journal, 737, 103
Schmidt, K. B., Treu, T., Trenti, M., et al. 2014, The Astrophysical Journal, 786, 57
Stefanon, M., Labbé, I., Bouwens, R. J., et al. 2017, The Astrophysical Journal, 851, 43
Suchkov, A., & Baggett, S. 2012, Instrument Science Report WFC3 2012-02
Trenti, M., Bradley, L. D., Stiavelli, M., et al. 2011, The Astrophysical Journal Letters, 727, L39
—. 2012, The Astrophysical Journal, 746, 55
van Dokkum, P. G. 2001, The Publications of the Astronomical Society of the Pacific, 113, 1420